Letter

Reducing Spontaneous Orientational Polarization via Semiconductor Dilution Improves OLED Efficiency and Lifetime

Emmanuel O. Afolayan,[1] Ibrahim Dursun,[1] Chao Lang,[2] Evgeny Pakhomenko,[3] Marina Kondakova,[4] Michael Boroson,[4] Michael Hickner,[2] Russell J. Holmes,[3] and Noel C. Giebink[1,*]

[1] *Department of Electrical Engineering, The Pennsylvania State University, Pennsylvania16802, USA*
[2] *Department of Material Science, The Pennsylvania State University, Pennsylvania 16802, USA*
[3] *Department of Chemical Engineering and Materials Science, University of Minnesota, Minneapolis 55455, USA*
[4] *OLEDWorks LCC, 1645 Lyell Ave., Rochester, New York 14606, USA*

(Received 17 February 2022; revised 12 April 2022; accepted 21 April 2022; published 26 May 2022)

Spontaneous orientational polarization (SOP) in the electron-transport layer (ETL) of organic light-emitting diodes (OLEDs) is increasingly recognized as a key factor influencing their performance. Here, we show that SOP is dramatically reduced in the common electron-transport material 2,2′,2″-(1,3,5-benzinetriyl)-tris(1-phenyl-1-*H*-benzimidazole) by coevaporating it together with medium-density polyethylene. Eliminating SOP from the ETL of blue fluorescent OLEDs in this manner reduces their operating voltage by 0.5 V, increases their external quantum efficiency (EQE) by 30%, and leads to a three-fold increase in device lifetime. We show that the EQE and lifetime improvements both originate from reduced exciton-polaron annihilation in the emissive layer, and that this leads to a functional relationship between the two quantities that can be used to quantify the rate of annihilation-induced degradation in the device. These results highlight a substantial opportunity to improve OLED performance by controlling SOP through semiconductor dilution and suggest that this capability can be used to systematically isolate and understand exciton-polaron degradation in the pursuit of stable blue OLEDs.

DOI: 10.1103/PhysRevApplied.17.L051002

Introduction.—Spontaneous orientational polarization (SOP) is an interesting phenomenon observed in many organic thin films, where the constituent molecules exhibit a net orientation of their permanent dipole moment [1,2]. This gives rise to a macroscopic polarization density (with corresponding surface potentials on the order of 0.05 V/nm) that, in turn, can influence the performance of devices such as organic light-emitting diodes (OLEDs) [1,3,4]. In particular, SOP is known to occur in many OLED electron-transport materials (ETMs) [3], where it induces a large hole density in the emissive layer that can alter electron injection from the cathode [5], shift the position of the recombination zone [1], and exacerbate exciton-polaron quenching (EPQ) [6–8].

While these effects can be avoided by choosing an ETM without SOP [6], the fact that so many otherwise high-performance ETMs possess SOP motivates interest in having a nonsynthetic pathway to control it. To this end, some control over SOP has been achieved by depositing materials at elevated substrate temperature [6,9]; however, the practical value of this strategy is limited by the requirement that the rest of the OLED stack also be stable at high temperature. Diluting ETM materials with nonpolar wide-energy-gap molecules offers another path to manipulate SOP (and potentially also improve charge transport [10]), yet efforts so far tend to enhance the molecular dipole orientation instead of eliminate it [11,12].

Here, we show that diluting the common ETM 2,2′,2′-(1,3,5-benzinetriyl)-tris(1-phenyl-1-*H*-benzimidazole) (TPBi) with medium-density polyethylene (MDPE) dramatically reduces its SOP without significantly affecting charge transport. In blue fluorescent OLEDs with a 20-nm-thick TPBi electron-transport layer (ETL), eliminating SOP in this fashion reduces the operating voltage by about 0.5 V, increases the external quantum efficiency (EQE) by about 30% (which together leads to a 50% increase in luminous efficacy), and leads to a threefold increase in device lifetime. We show that both the EQE and lifetime improvement stem from reduced EPQ in the emissive layer (EML) owing to a decrease in the excess hole density that is normally induced by SOP. These results highlight a substantial opportunity to improve OLED performance by controlling SOP and suggest that this capability can be used as a diagnostic tool to quantify the impact of EPQ on OLED operational degradation.

*ncg2@psu.edu

Experimental methods.—The OLEDs studied in this work are fabricated at OLEDWorks LLC via vacuum thermal evaporation on prepatterned, 150-nm-thick indium tin oxide (ITO) glass substrates using sublimation-purified TPBi, 4,6-bis(3,5-di-3-pyridylphenyl)-2-methylpyrimidine (B3PyMPM), 1,4-bis(triphenylsilyl)benzene (UGH2), and N,N-di(1-naphthyl)-N,N-diphenyl(1,1-biphenyl)-4,4-diamine (NPB); the remaining EML (a blue fluorescent guest:host system doped at 4 wt %) and electron-blocking (EBL) and hole-blocking (HBL) layers in the device are proprietary. MDPE is purchased from Sigma Aldrich (product number 427 772, $M_w \sim 4000$, $M_n \sim 1700$) and used as received; it is degassed in the boat for 10 min prior to evaporation. The chemical, morphological, and electrical characteristics of evaporated polyethylene films are described in Ref. [13]. The full device structure consists of ITO/p-doped NPB(10 nm)/NPB(200 nm)/EBL(10 nm)/EML(20 nm)/HBL(10 nm)/ETL(20 nm)/Li:TPBi(5 nm)/Yb(0.8 nm)/Ag (140 nm) and has a lit area of 0.1 cm^2. The devices are packaged in a N_2 glove box using a glass cover with an edge bead of epoxy.

Current-voltage-luminance characteristics are measured using a Photo Research PR655 spectral radiometer and source-measure unit, while fade testing is conducted at constant current at an ambient temperature of 25 °C. Capacitance-voltage measurements are carried out at a frequency of 10 kHz with a Zurich Instruments impedance analyzer using a 30 mV rms ac dither. Bias-dependent photoluminescence is measured via the synchronous detection method described in Refs. [6,8,13,14] using $\lambda = 405$ nm laser light (incident at 45° with an intensity of approximately 16 mW cm^{-2}) that is primarily absorbed in the EML, resulting in a PL spectrum that closely matches the EL spectrum, as shown in the Supplemental Material [15].

Transfer matrix-based optical and drift-diffusion electrical modeling of the devices is carried out using the SETFOS software package from Fluxim AG [16–19]. The optical constants of each layer are determined from spectroscopic ellipsometry, whereas the electrical parameters are estimated from the literature. The effect of SOP is modeled by introducing sheet charge densities with opposite polarity on either side of the ETL following the approach described in Ref. [20]; full details of the model and its parameters are provided in the Supplemental Material [15].

Results and discussion.—Figure 1(a) summarizes the luminance-current density-voltage characteristics of three fluorescent blue OLEDs that differ only in their 20-nm-thick ETL [see Fig. 1(b), inset, for the full device structure], which consists either of neat TPBi, TPBi coevaporated with 30 wt % of the wide-gap host material UGH2, or TPBi coevaporated with 30-wt % MDPE [21]. Whereas diluting with UGH2 leads to a slight voltage increase that is expected from blending with an insulator, adding MDPE reduces the OLED operating voltage by about 0.5 V. Moreover, Fig. 1(b) shows that the MDPE-diluted device also exhibits a significantly higher EQE compared with the neat TPBi and UGH2-diluted devices. Taken together, the EQE increase and voltage reduction achieved by diluting with MDPE yield about a 50% boost in luminous efficacy at 100 cd/m^2, which is significant for an otherwise optimized blue OLED.

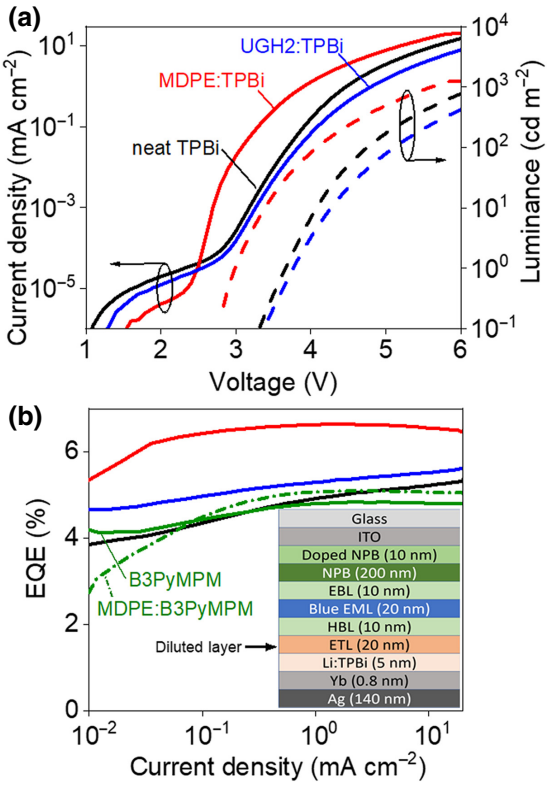

FIG. 1. (a) Current density–voltage–luminance characteristics for devices with neat TPBi (black), 30-wt % MDPE:TPBi (red), and 30-wt % UGH2:TPBi (blue) ETLs. (b) EQE of the devices from (a), together with that from two additional devices incorporating the nonpolar ETL material B3PyMPM (solid green curve) and 30-wt % MDPE:B3PyMPM (dashed green curve) for comparison. Inset, schematic of the blue OLED architecture; only the composition of the ETL is varied between devices. Other layers in the device include the hole-transport material NPB, as well as proprietary EML, EBL, and HBL layers.

The reported EQE increase is not an optical effect associated with the lower refractive index of the MDPE:TPBi blend ($n_{\mathrm{TPBi}} = 1.71$ and $n_{\mathrm{MDPE}} = 1.49$), as there is no change in emission spectrum between the devices, and dipole-emission modeling in the Supplemental Material [15] predicts a negligible change in outcoupling efficiency. Drift-diffusion simulations similarly rule out the lower electron mobility of MDPE:TPBi (roughly half that of neat TPBi [22]) as the cause of the EQE increase; see the Supplemental Material for details [15]. This is consistent with the fact that the UGH2-diluted

device, which has a similar mobility reduction, does not exhibit an increased EQE. Given that the diluted layer is not in direct contact with the emissive layer, and there is no reason to expect a shift in TPBi energy levels upon adding MDPE or UGH2, exciton confinement and injection into the emissive layer should also remain unchanged.

Interestingly, however, Fig. 1(b) shows that, if TPBi is replaced with an ETM, such as B3PyMPM, that does not possess SOP, diluting with MDPE yields no EQE improvement (or reduction in drive voltage; not shown). In light of recent work by Bangsund *et al.* [6], who showed that SOP is responsible for a higher rate of EPQ in TPBi-based devices, the results of Fig. 1(b) suggest that the beneficial effect of MDPE in TPBi may result from reducing its SOP.

Capacitance-voltage (*C-V*) measurements shown in Fig. 2(a) support this hypothesis, demonstrating a positive shift in the transition voltage of the MDPE:TPBi device relative to the others. This transition voltage, which corresponds to the onset of hole injection in the device as sketched in the inset (i.e., the capacitance increases when charge is only modulated across the HBL and ETL layers instead of the entire device thickness), decreases linearly with increasing SOP [3]. Measuring the change in *C-V* transition voltage as a function of ETL thickness for a series of bilayer devices in the Supplemental Material [15], we find that the charge density accumulated in response to SOP for 30-wt % MDPE:TPBi [(0.09 ± 0.02) mC m^{-2}] is over 20 times lower than that of neat TPBi [(1.98 ± 0.02) mC m^{-2}].

Figure 2(b) shows that the SOP-induced change in *C-V* transition voltage correlates with a decrease in the EML photoluminescence (PL) quantum yield of each device. As in Ref. [6], we attribute this behavior to EPQ that stems from the large density of holes induced at the EML/HBL interface by the SOP in TPBi. Support for this interpretation follows from the drift-diffusion modeling results presented in Fig. 3, which reproduce all of the qualitative changes caused by MDPE dilution, including the reduction in drive voltage [Fig. 3(a)], the increase in EQE [Fig. 3(b)], the increase in *C-V* transition voltage [Fig. 3(c)], and the reduction in PL quenching [Fig. 3(d)]. The simulations are carried out on the layer stack from Fig. 1(a) using SETFOS, with SOP densities of 2.0 mC m^{-2} (TPBi) and 0.09 mC m^{-2} (MDPE:TPBi) implemented in the ETL following the approach taken in Ref. [20]. The reduction in drive voltage for MDPE:TPBi originates from the smaller SOP-induced potential drop across the ETL (see the band diagram in the Supplemental Material [15]), which enables electron injection and drift through this layer to begin at lower applied bias. The difference in EQE and PL quenching between the two simulations originates solely from different levels of EPQ (a bimolecular rate coefficient of $K_{XP} = 10^{-11}$ cm^3 s^{-1} is assumed in the EML; XP stands for exciton-polaron) due to the SOP-induced hole density, as detailed in the Supplemental Material [15]. Reasonable

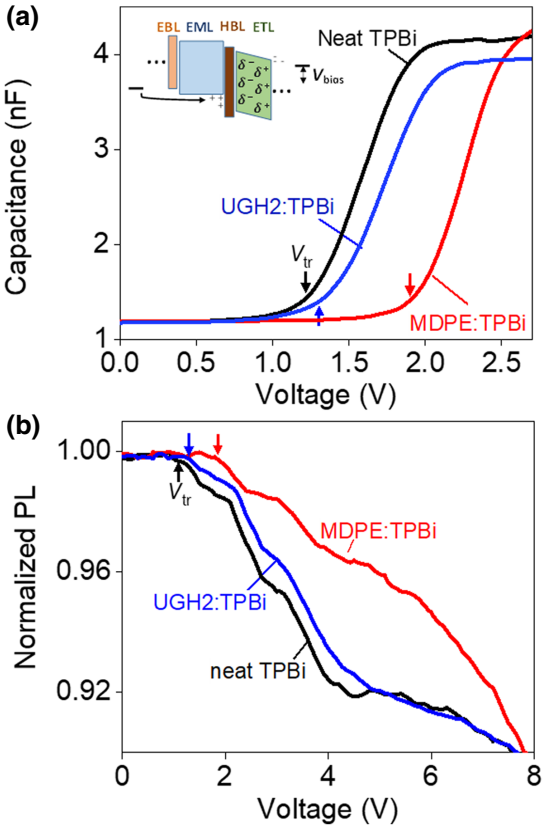

FIG. 2. (a) Capacitance–voltage data for the blue OLEDs from Fig. 1(a). The increase in capacitance, which is associated with the onset of hole injection into the emissive layer illustrated in the inset (δ^+ and δ^- denote the SOP-bound charge in the ETL), shifts to higher bias when TPBi is diluted with UGH2 and MDPE. (b) Emissive-layer PL quantum yield for each device (normalized to its value at short circuit), demonstrating that the onset voltage of PL quenching scales with the capacitance transition in (a). Data are collected with a chopped $\lambda = 405$ nm excitation beam (which selectively excites the blue-fluorescent dopant in the EML) using the synchronous detection method from Refs. [6,13] to reject background electroluminescence. Colored arrows in both plots indicate the transition voltage that marks the onset of hole injection determined from the capacitance-voltage data in (a).

agreement between the simulated and experimental EQE and PL quenching results, as well as an independent ratiometric analysis of the two quantities provided in the Supplemental Material [15], strongly support the conclusion that the EQE improvement realized from diluting with MDPE is due to reduced EPQ.

In addition to improved device performance, Fig. 4(a) shows that the MDPE:TPBi device degrades much more slowly than its neat TPBi and UGH2:TPBi counterparts (driven at equal current density), resulting in more than a threefold increase in lifetime (to 90% of initial luminance, T_{90}). Since these devices are virtually identical, except for the magnitude of the SOP-induced hole concentration in

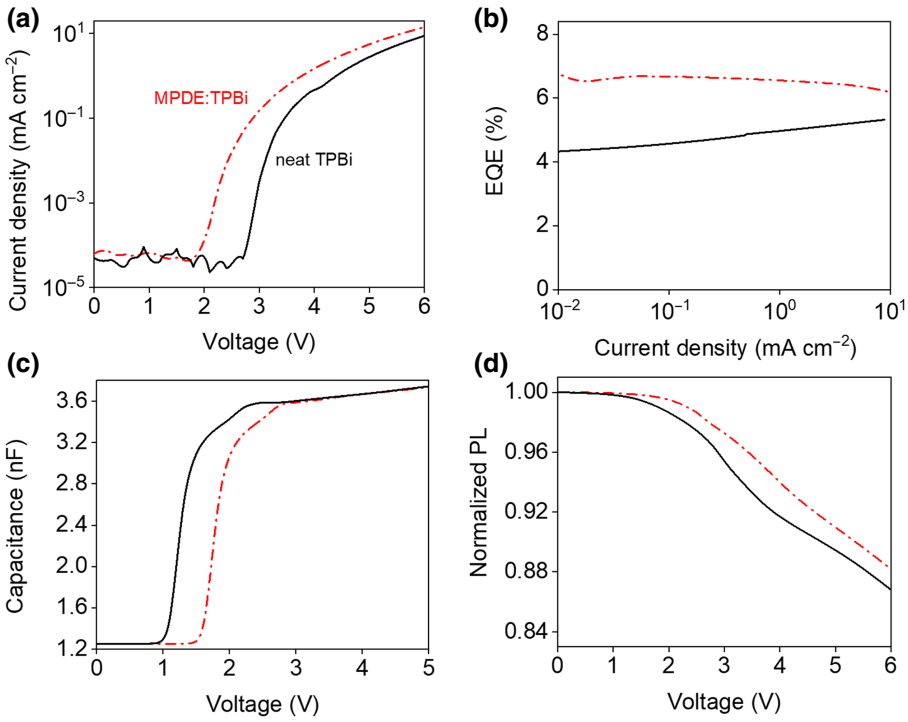

FIG. 3. Simulated current–voltage (a), external quantum efficiency (b), capacitance–voltage (c), and normalized photoluminescence quenching (d) characteristics of the TPBi (solid curves) and MDPE:TPBi (dotted-dashed curves) devices using a SETFOS drift-diffusion model. The only difference between the two devices is the polarization charge built into their ETL, which is 2.0 mC m^{-2} for the TPBi device and 0.09 mC m^{-2} for the MDPE:TPBi device based on the giant surface potential slopes measured in the Supplemental Material [15]. The difference in EQE and PL quenching behavior between the devices is due to EPQ with holes based on a rate coefficient of $K_{XP} = 10^{-11}$ cm^3 s^{-1}; full details on the model and the parameters used in it are provided in the Supplemental Material [15].

their EMLs, it seems reasonable to conclude that holes (i.e., molecular cations) play a role in the chemical degradation process that takes place there. Indeed, previous work [23,24] has established that molecular degradation in devices with SOP concentrates in the EML at the location of the SOP-induced hole density (i.e., adjacent to the EML/HBL interface). These studies postulated that degradation originates from the instability of excitons in the EML; however, this cannot be the primary mechanism in our case, since the exciton density (and thus, any exciton-driven degradation rate) of all three devices is similar based on their initial luminance. We rule out direct instability of cationic host or dopant molecules based on the fact that the shelf life of the devices does not differ (i.e., does not correlate with the large difference in their equilibrium hole concentration shown in the Supplemental Material [15]), which leaves bimolecular EPQ-driven degradation [25,26] as the most likely mechanism. This is not to say that other modes of degradation do not take place in parallel (and in other layers of the device as well) [27,28], only that the change in lifetime from MDPE dilution is tied to the change in EPQ originating from the lower SOP-induced hole density in the EML, since this is the primary difference established between these devices.

Given that the EQE difference between these devices is also attributed to EPQ, this degradation hypothesis implies that their EQEs and lifetimes should be correlated. The Supplemental Material [15] formalizes this notion, showing that $T_{90} \propto [J(\chi\phi_{PL0} - \eta_{IQE})]^{-1}$ in OLEDs where EPQ is the principal driver of both internal quantum efficiency (IQE) loss and molecular degradation in the EML. In this expression, ϕ_{PL0} is the PL quantum yield of the pristine EML (i.e., in the absence of EPQ and degradation); χ is the radiative exciton spin fraction; and η_{IQE} is the IQE of the pristine OLED at the fade current density, J.

Figure 4(b) plots the lifetime of each device versus its EQE for the two fade current densities, demonstrating that this EPQ scaling relationship describes the data remarkably well based on the known singlet spin fraction ($\chi = 0.25$), outcoupling efficiency ($\eta_{EQE} = 0.3\eta_{IQE}$; see the Supplemental Material [15]), and PL quantum yield ($\phi_{PL0} = 0.95$) of the device. We note that, at sufficiently high current, the injected hole density will eventually overwhelm that due to SOP, which, in turn, would be expected to eliminate the lifetime difference between the TPBi and MDPE:TPBi devices. The point at which this occurs would correspond to the current density where the two EQEs converge (since their difference is attributed solely to EPQ from the SOP-induced excess hole density), which is higher than the 20 mA cm^{-2} maximum used in our fade measurements, according to Fig. 1(b). The model in Fig. 4(b) naturally includes this high-current regime, since, when the EQEs become equal, so do the lifetimes.

While more data from devices with varying SOP (e.g., more dilution concentrations) and different fade currents would be required to rigorously fit this model, the results in Fig. 4(b) are sufficiently compelling to motivate the use of dilution-controlled SOP as a diagnostic tool to determine whether EPQ degradation is significant in a given device architecture. This is notoriously difficult to determine based on standard performance and lifetime data [25], but it is important for guiding the development of

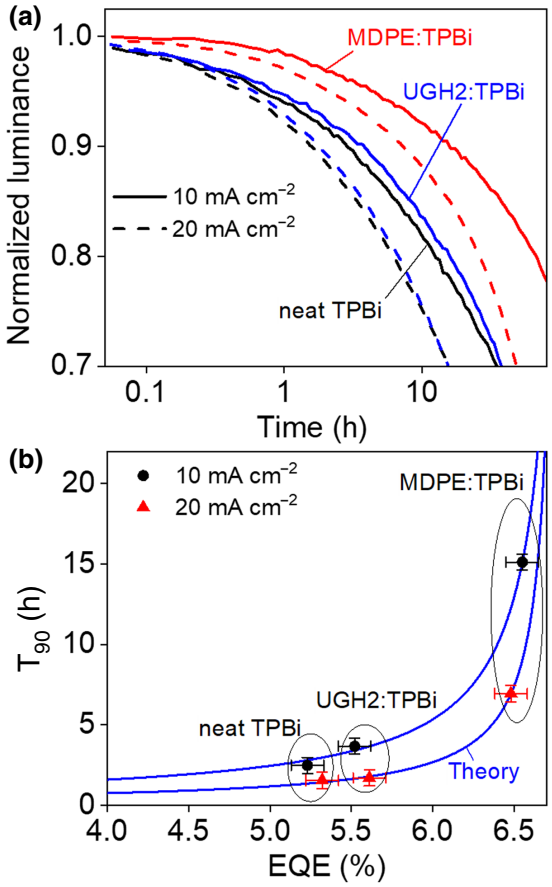

FIG. 4. (a) Luminance fade results for the TPBi, UGH2:TPBi and MDPE:TPBi OLEDs at constant current densities of $J = 10$ and 20 mA cm^{-2}. (b) Degradation lifetime (to 90% of initial luminance) plotted as a function of initial EQE at the fade current density, demonstrating the EPQ scaling relationship (blue lines) presented in the text.

a long-lived blue phosphorescent (or thermally activated delayed fluorescence) EML formulation, which remains an elusive goal for the OLED industry.

In this context, it is worth considering why MDPE is so much more effective than UGH2 at suppressing SOP in TPBi (as well as other common ETL materials; see the Supplemental Material [15]). The answer is likely related to different steric effects, where a compact molecule such as UGH2, can pack in the TPBi matrix with minimal disruption, while the flexible MDPE chain fragments possess active radicals and can partially repolymerize, forming a fibrous network around TPBi molecules that restricts their natural orientational alignment. Similar networks are known to form in the case of other coevaporated polymer–small-molecule blends [29,30], where the restricted molecular motion manifests in an increased glass-transition temperature [29]. The disruptive effect of MDPE on molecular orientation is also evident from ellipsometry, where it eliminates the normally anisotropic refractive index of molecules such as B3PyMPM [31]; see the Supplemental Material [15] for details.

These observations suggest that a dilution molecule, purposely built to frustrate SOP (as opposed to the random chain fragments that result from thermal evaporation of a polymer), might take the form of an aliphatic oligomer, with low enough molecular weight to evaporate and form a fibrous network in the deposited film, yet large enough not to spontaneously sublime under vacuum. With a better understanding of the minimum concentration needed to frustrate SOP while preserving charge-carrier mobility [29], such a dilution molecule could provide a powerful solution for controlling SOP in the many OLEDs that possess it.

Conclusion.—We show that the SOP in TPBi can be virtually eliminated by diluting with MDPE, and that this significantly improves the efficiency and lifetime of blue OLEDs that employ a TPBi electron-transport layer. Both changes stem from a decrease in EPQ owing to fewer excess holes in the recombination zone, which results in a correlation between EQE and lifetime that can be used to quantify EPQ degradation in the EML. Given that SOP is significant in most OLED ETMs, the capability to control it via semiconductor dilution has the potential not only to benefit many existing devices, but also to systematically isolate and understand EPQ-driven operational degradation in the pursuit of longer-lived blue OLEDs.

Acknowledgments.—This work is supported by the US Department of Energy (DOE) EERE SSL program under Award No. DE-EE0008717. R.J.H. and E.P. acknowledge support from Ronald L. and Janet A. Christenson and the Robert and Beverly Sundahl Fellowship.

[1] Y. Noguchi, W. Brütting, and H. Ishii, Spontaneous orientation polarization in organic light-emitting diodes, Jpn. J. Appl. Phys. **58**, SF0801 (2019).

[2] Y. Ueda, H. Nakanotani, T. Hosokai, Y. Tanaka, H. Hamada, H. Ishii, S. Santo, and C. Adachi, Role of spontaneous orientational polarization in organic donor–acceptor blends for exciton binding, Adv. Opt. Mater. **8**, 2000896 (2020).

[3] Y. Noguchi, Y. Miyazaki, Y. Tanaka, N. Sato, Y. Nakayama, T. D. Schmidt, W. Brütting, and H. Ishii, Charge accumulation at organic semiconductor interfaces due to a permanent dipole moment and its orientational order in bilayer devices, J. Appl. Phys. **111**, 114508 (2012).

[4] Y. Noguchi, K. Osada, K. Ninomiya, H. D. C. N. Gunawardana, K. R. Koswattage, and H. Ishii, Influence of intermolecular interactions on the formation of spontaneous orientation polarization in organic semiconducting films, J. Soc. Inf. Disp. **29**, 29 (2021).

[5] Y. Noguchi, H. Lim, T. Isoshima, E. Ito, M. Hara, W. W. Chin, J. W. Han, H. Kinjo, Y. Ozawa, Y. Nakayama,

and H. Ishii, Influence of the direction of spontaneous orientation polarization on the charge injection properties of organic light-emitting diodes, Appl. Phys. Lett. **102**, 203306 (2013).

[6] J. S. Bangsund, J. R. Van Sambeek, N. M. Concannon, and R. J. Holmes, Sub–turn-on exciton quenching due to molecular orientation and polarization in organic light-emitting devices, Sci. Adv. **6**, eabb2659 (2020).

[7] A. P. Marchetti, T. L. Haskins, R. H. Young, and L. J. Rothberg, Permanent polarization and charge distribution in organic light-emitting diodes (OLEDs): Insights from near-infrared charge-modulation spectroscopy of an operating OLED, J. Appl. Phys. **115**, 114506 (2014).

[8] T. Yamanaka, H. Nakanotani, and C. Adachi, Slow recombination of spontaneously dissociated organic fluorophore excitons, Nat. Commun. **10**, 5748 (2019).

[9] Y. Esaki, M. Tanaka, T. Matsushima, and C. Adachi, Active control of spontaneous orientation polarization of tris(8-hydroxyquinolinato)aluminum (Alq3) films and its effect on performance of organic light-emitting diodes, Adv. Electron. Mater. **7**, 2100486 (2021).

[10] D. Abbaszadeh, A. Kunz, G. A. H. Wetzelaer, J. J. Michels, N. I. Crăciun, K. Koynov, I. Lieberwirth, and P. W. M. Blom, Elimination of charge carrier trapping in diluted semiconductors, Nat. Mater. **15**, 628 (2016).

[11] H. D. C. N. Gunawardana, K. Osada, K. R. Koswattage, and Y. Noguchi, Enhancement of the molecular orientation of TPBi in coevaporated films of UGH-2 host molecules, Surf. Interface Anal. **53**, 460 (2021).

[12] L. Jäger, T. D. Schmidt, and W. Brütting, Manipulation and control of the interfacial polarization in organic light-emitting diodes by dipolar doping, AIP Adv. **6**, 095220 (2016).

[13] Y. Shirasaki, G. J. Supran, W. A. Tisdale, and V. Bulović, Origin of Efficiency Roll-Off in Colloidal Quantum-Dot Light-Emitting Diodes, Phys. Rev. Lett. **110**, 217403 (2013).

[14] W. Zou, R. Li, S. Zhang, Y. Liu, N. Wang, Y. Cao, Y. Miao, M. Xu, Q. Guo, D. Di, L. Zhang, C. Yi, F. Gao, R. H. Friend, J. Wang, and W. Huang, Minimising efficiency roll-off in high-brightness perovskite light-emitting diodes, Nat. Commun. **9**, 608 (2018).

[15] See the Supplemental Material at http://link.aps.org/supplemental/10.1103/PhysRevApplied.17.L051002 for supporting data and derivations.

[16] A. Sharma and T. D. Das, Light extraction efficiency analysis of fluorescent OLEDs device, Opt. Quantum Electron. **53**, 83 (2021).

[17] S. Altazin, L. Penninck, B. Ruhstaller, in *Handbook of Organic Light-Emitting Diodes*, edited by C. Adachi, *et al.* (Springer Japan, Tokyo, 2018), p. 1.

[18] J.-H. Jou, J.-W. Weng, S. D. Chavhan, R. A. K. Yadav, and T.-W. Liang, Investigation of charge-transporting layers for high-efficiency organic light-emitting diode, J. Phys. D: Appl. Phys. **51**, 454002 (2018).

[19] U. Aeberhard, S. Zeder, and B. Ruhstaller, Reconciliation of dipole emission with detailed balance rates for the simulation of luminescence and photon recycling in perovskite solar cells, Opt. Express **29**, 14773 (2021).

[20] S. Altazin, S. Züfle, E. Knapp, C. Kirsch, T. D. Schmidt, L. Jäger, Y. Noguchi, W. Brütting, and B. Ruhstaller, Simulation of OLEDs with a polar electron transport layer, Org. Electron. **39**, 244 (2016).

[21] T. Kim, E. Afolayan, C. J. Ruud, H. Kim, J. S. Price, A. Brigeman, Y. Shen, and N. C. Giebink, Electrical injection and transport in Teflon-diluted hole transport materials, Org. Electron. **83**, 105754 (2020).

[22] Y. Wang, B. Li, C. Jiang, Y. Fang, P. Bai, and Y. Wang, Study on electron transport characterization in TPBi thin films and OLED application, J. Phys. Chem. C **125**, 16753 (2021).

[23] T. D. Schmidt, L. Jäger, Y. Noguchi, H. Ishii, and W. Brütting, Analyzing degradation effects of organic light-emitting diodes via transient optical and electrical measurements, J. Appl. Phys. **117**, 215502 (2015).

[24] Y. Noguchi, H.-J. Kim, R. Ishino, K. Goushi, C. Adachi, Y. Nakayama, and H. Ishii, Charge carrier dynamics and degradation phenomena in organic light-emitting diodes doped by a thermally activated delayed fluorescence emitter, Org. Electron. **17**, 184 (2015).

[25] N. C. Giebink, B. W. D'Andrade, M. S. Weaver, P. B. Mackenzie, J. J. Brown, M. E. Thompson, and S. R. Forrest, Intrinsic luminance loss in phosphorescent small-molecule organic light emitting devices due to bimolecular annihilation reactions, J. Appl. Phys. **103**, 044509 (2008).

[26] N. C. Giebink, B. W. D'Andrade, M. S. Weaver, J. J. Brown, and S. R. Forrest, Direct evidence for degradation of polaron excited states in organic light emitting diodes, J. Appl. Phys. **105**, 124514 (2009).

[27] S.-C. Dong, L. Xu, and C. W. Tang, Chemical degradation mechanism of TAPC as hole transport layer in blue phosphorescent OLED, Org. Electron. **42**, 379 (2017).

[28] W. Song, J. Y. Lee, T. Kim, Y. Lee, and H. Jeong, Comprehensive understanding of degradation mechanism of high efficiency blue organic light-emitting diodes at the interface by hole and electron transport layer, Org. Electron. **57**, 158 (2018).

[29] Price J. S. Price, B. Wang, T. Kim, A. J. Grede, J. M. Sandoval, R. Xie, Y. Shen, D. R. Adams, M. J. Eller, A. Sokolov, S. Mukhopadhyay, P. Trefonas, E. D. Gomez, E. A. Schweikert, and N. C. Giebink, Fluoropolymer-diluted small molecule organic semiconductors with extreme thermal stability, Appl. Phys. Lett. **113**, 263302 (2018).

[30] B. Wang, C. J. Ruud, J. S. Price, H. Kim, and N. C. Giebink, Graded-index fluoropolymer antireflection coatings for invisible plastic optics, Nano Lett. **19**, 787 (2019).

[31] H. Shin, J.-H. Lee, C.-K. Moon, J.-S. Huh, B. Sim, and J.-J. Kim, Sky-blue phosphorescent OLEDs with 34.1% external quantum efficiency using a low refractive index electron transporting layer, Adv. Mater. **28**, 4920 (2016).